An application of a large scale conceptual hydrological model over the Elbe region

M. Lobmeyr, D. Lohmann, C. Ruhe

Hydrology and Earth System Sciences, 3(3), *363–374* (1999) © EGS

Hydrology & Earth System Sciences

An application of a large scale conceptual hydrological model over the Elbe region

Manfred Lobmeyr*[1], Dag Lohmann[2] and Cord Ruhe[1]

[1] GKSS Research Center Geesthacht, Institute for Atmospheric Physics D-21502 Geesthacht, Germany.
[2] Department of Civil Engineering and Operations Research, Princeton University, Princeton, 08540, NJ, USA.
* e-mail address for corresponding author: lobmeyr@gkss.de.

Abstract

This paper investigates the ability of the VIC-2L model coupled to a routing model to reproduce streamflow in the catchment of the lower Elbe River, Germany. The VIC-2L model, a hydrologically-based land surface scheme (LSS) which has been tested extensively in the Project for Intercomparison of Land-surface Parameterization Schemes (PILPS), is put up on the rotated grid of 1/6 degree of the atmospheric regional scale model (REMO) used in the Baltic Sea Experiment (BALTEX). For a 10 year period, the VIC-2L model is forced in daily time steps with measured daily means of precipitation, air temperature, pressure, wind speed, air humidity and daily sunshine duration. VIC-2L model output of surface runoff and baseflow is used as input for the routing model, which transforms modelled runoff into streamflow, which is compared to measured streamflow at selected gauge stations. The water balance of the basin is investigated and the model results on daily, monthly and annual time scales are discussed. Discrepancies appear in time periods where snow and ice processes are important. Extreme flood events are analyzed in more detail. The influence of calibration with respect to runoff is examined.

Introduction

An understanding of the water and energy budgets at the land surface plays an important role in predicting the future climate, forecasting the weather and estimating water resources. The interface between the atmosphere and the land surface is modelled by land-surface schemes (LSS), which are currently tested off- and on-line in the Project for Intercomparison of Land-Surface Parameterization Schemes (PILPS, Henderson-Sellers and Hopkins, 1998) and also in the Global Soil Wetness Project (GSWP, 1998). Most of these LSS have very detailed descriptions of their energy budget, while the soil hydrology, especially the upper (infiltration) and lower (baseflow) boundary condition, is treated rather poorly. Because energy and water budgets are connected through evapotranspiration (or latent heat flux), an inadequate representation in one of the budgets may lead to errors in the other. A recent investigation within the PILPS phase 2(c) (Wood *et al.*, 1998; Liang *et al.*, 1998; Lohmann *et al.*, 1998) of the water budget of the Red-Arkansas River showed very large differences in the runoff production mechanisms of LSS, which resulted in very distinct modelled streamflow time series. The timing of modelled runoff (and therefore streamflow) showed that some basic model assumptions (e.g. free drainage lower boundary condition or high homogeneous infiltration capacity) are inaccurate and the corresponding parameterizations are open to improvement. On the other hand, operational lumped conceptual hydrological models, like the Sacramento model (Burnash, 1995), are able to reproduce streamflow of large river basins. However, their treatment of the energy balance as well as their inadequacy to work at small time steps is not compatible with the strict requirements of atmospheric models. It is concluded that the most appropiate method includes realistic runoff production mechanisms in the LSS, rather than modify the hydrological model to work as a LSS.

This paper investigates the ability of the hydrologically-based VIC-2L (Liang *et al.*, 1994) LSS coupled to a routing model (Lohmann *et al.*, 1996) to reproduce streamflow of the Elbe River, Germany. Daily atmospheric measurements over 10 years (precipitation, air temperature, pressure, wind speed, air humidity and sunshine duration) by the German Weather Service (DWD) were used to force the VIC-2L model offline in its water balance mode. The forcing data were gridded to the rotated grid of 1/6 degree (*ca.* 18×18 km^2) of the atmospheric regional scale model REMO (Karstens *et al.*, 1996), which is used in the BALTEX project (Raschke *et al.*, 1998). Conceptually, vertical processes are described by the VIC-2L model, which includes evapotranspiration, surface runoff and

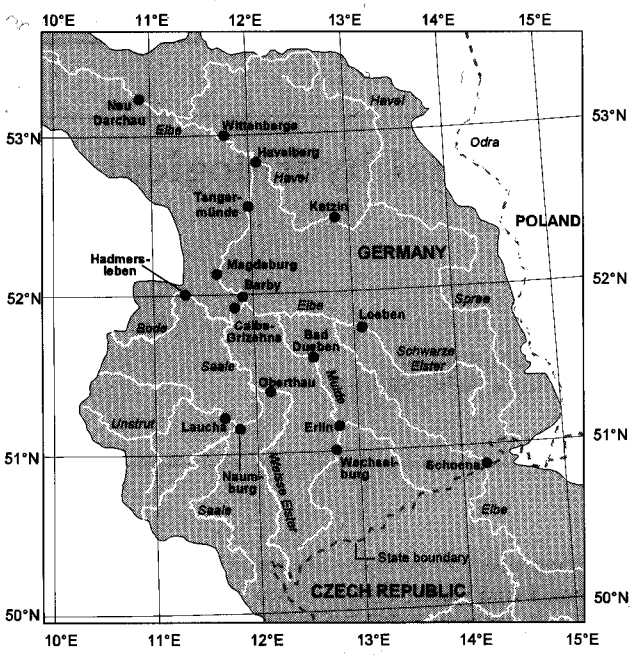

Fig. 1. *Elbe Catchment with main tributaries and gauge stations.*

baseflow generation. Horizontal water movement is divided into transport processes inside a grid box and transport processes within the river system; both are described by linear functions (Lohmann *et al.*, 1996, 1998a). The calibration was done on 1 year's data. The model was then forced with the remaining 9 years of atmospheric data and measured and predicted time series of stream flow were compared. The model is applied over a main part of the Elbe region and a comparison is made with measured discharge at 13 gauge stations within the basin.

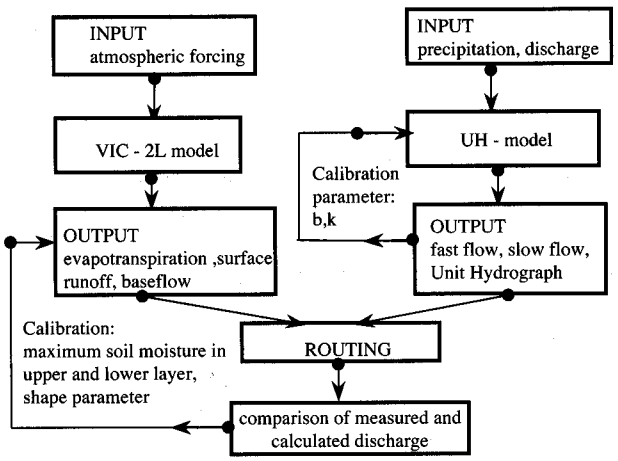

Fig. 2. *Model setup and calibration procedure.*

Model concept

The model consists of two independent parts, a vertical land surface scheme (LSS) and a horizontal routing scheme (Fig. 2). The VIC-2L model calculates the vertical energy and water fluxes and represents the state of the system (e.g. temperature and soil moisture). The horizontal routing model is used to transport VIC-2L produced surface runoff and baseflow (Lohmann *et al.*, 1998a).

THE LAND SURFACE SCHEME

The VIC-2L model (Liang, 1994; Liang *et al.*, 1994) is a two layer LSS for general circulations models and numerical weather prediction models. It has participated in the PILPS experiments (Henderson-Sellers *et al.*,1995; Chen *et al.*, 1997; Wood *et al.*, 1998) as well as in a number of large scale hydrological studies (Nijssen *et al.*, 1997; Lohmann *et al.*, 1998a, b). Its most distinguishing features compared to other LSS are the surface runoff (Wood *et al.*, 1992) and baseflow parametrizations (Francini and Pacciani, 1991), which also have been used in flood forecast, (see O'Connell and Todini, 1996 and references therein). The spatial distribution of the infiltration capacity in each grid box is given by:

$$i = i_m[1 - (1 - A)^{1/s}] \tag{1}$$

where i_m is the maximum infiltration capacity, i the actual infiltration capacity, A is the area fraction of the grid box with an infiltration capacity smaller than i, and s is the shape parameter which is obtained by calibration. The integral of i over the entire area is the maximum storage capacity of the upper soil layer (see Wood *et al.*, 1992). The response of surface runoff Q^{surf} to a precipitation event P is calculated from:

$$Q^{surf} = \begin{cases} P + W_1 - W_1^{\max} & i + P \geq i_m \\ P + W_1 - W_1^{\max}\left[1 - \left(1 - \dfrac{i + P}{i_m}\right)^{1+s}\right] & i + P < i_m \end{cases} \tag{2}$$

W_1^{max} is the maximum water content of the upper layer, W_1 is the actual water content. Percolation from the upper to the lower layer is driven only by gravity with the help of the Brooks—Corey relationship (Brooks and Corey, 1988), to estimate the hydraulic conductivity. Baseflow Q^{base} is represented by the Arno scheme (Francini and Pacciani, 1991, Todini 1996):

$$Q^{base} = \begin{cases} d_1 W_2 & W_2 \leq W_2^S W_2^{\max} \\ d_1 W_2 + d_2 (W_2 - W_2^S W_2^{\max})^K & W_2 > W_2^S W_2^{\max} \end{cases} \tag{3}$$

where W_2 is the actual water content of the lower soil layer, W_2^{max} is the maximum soil water content, W_2^S is the fraction of the maximum soil water content at which the baseflow curve becomes nonlinear, d_1 is the storage con-

stant for the linear part, d_2 is the storage constant for the nonlinear part of the baseflow curve and K is the shape of the non-linear part of the baseflow curve. Maximum soil water content is dependent on the soil type, although in this study it was obtained by calibration. For each vegetation type, characteristics, such as leaf area index, canopy resistance, roughness length and displacement height are prescribed. Evapotranspiration is calculated with the Penman-Monteith equation (e.g. Shuttleworth, 1993). The actual evapotranspiration is dependent on environmental stress factors related to soil moisture, vapour pressure deficit and air temperature following Noilhan and Planton (1989). Each grid cell can have partial coverage with different types of vegetation and bare soil. The total actual evaporation is calculated as the sum of canopy evaporation, evapotranspiration from each vegetation class and bare soil evaporation. To deal with snow processes, a temperature index model is used (Gray and Prowse, 1993).

ROUTING MODEL

The routing model (Lohmann *et al.*, 1996; Lohmann *et al.*, 1998a) describes the time for runoff to reach the outlet of a grid box, as well as the water transport in a river network. The basic assumption is that all horizontal routing processes are linear and time invariant. The time delay before locally produced runoff reaches the outlet of a grid cell is characterized by an impulse response function, or Unit Hydrograph, which is calculated by an iterative procedure (Duband *et al.*, 1993; Lohmann *et al.*, 1996). However, the VIC-2L parametrizations imply two different time scales of runoff productions, a fast surface component and a delayed baseflow component. The construction of the routing model will reflect these different time scales with a separation of the total measured streamflow into a fast and a slow component. This is done with a linear model formulation, proposed by Rodriguez (Rodriguez, 1989; Duband *et al.*, 1993):

$$\frac{dQ^S(t)}{dt} = -kQ^S(t) + bQ^F(t) \tag{4}$$

where $Q^S(t)$ is the slow flow, $Q^F(t)$ is the fast flow and $Q(t)$ is the total measured flow. $Q^S(t)$ and $Q^F(t)$ conceptually reflect the different time scales of $Q^{surf}(t)$ and $Q^{base}(t)$ in the VIC-2L model, although the correspondence is not 1:1. With discrete data, Eqn. 4 can be solved by:

$$Q^s(t) = \frac{\exp(-k\Delta t)}{1+b\Delta t} Q^s(t-\Delta t) + \frac{b\Delta t}{1+b\Delta t} Q(t) \tag{5}$$

Assuming a linear and time invariant relationship between the fast component of streamflow and part of the precipitation, called effective precipitation P^{eff}, a solution can be calculated for the impulse response function UH^F for the fast flow and P^{eff}. Both are determined by the following integral equation, which can be solved with an iterative procedure (Duband *et al.*, 1993 Lohmann *et al.*, 1996):

$$Q^F(t) = \int_0^T UH^F(\tau) P^{eff}(t-\tau) d\tau \tag{6}$$

where T is the length of impulse response function. Following Duband *et al.* (1993) for each iteration there are two constraints; the first is the non-negativity of all variables, the second simply states that effective precipitation is always less than or equal to the precipitation itself.

River transport is formulated with the linearized St. Venant's equation (Fread, 1993; Gupta *et al.*, 1986).

$$Q^R(x,t) = \int_0^T I(0,t-\tau) UH^R(x,\tau) d\tau \tag{7}$$

with

$$UH^R(x,t) = \frac{x}{2t\sqrt{\pi t D}} \exp\left(-\frac{(Ct-x)^2}{4Dt}\right) \tag{8}$$

$Q^R(x,t)$ means river discharge at each point x and each time step t as response function for the time varying discharge input $I(0,t)$ as upstream boundary condition. Values for the velocity C and diffusivity D can be found with the help of river geometry data (Moussa and Bocquillon, 1996), or with the help of least square optimization between neighbouring gauge stations (Lohmann *et al.*, 1996). In this work, river geometry data have been taken at selected gauges. For each grid cell, the Unit Hydrograph is calculated as a convolution of the grid box and river flow impulse response functions downstream from that grid cell.

Model application and setup

The model area contains the German part of the Elbe river basin above the gauge station Neu-Darchau with the subcatchments Saale, Mulde, Schwarze Elster and Havel-Spree of about 80000 km² (Fig. 1). It is the last gauge with measured discharge, upstream the tidal part of the Elbe river, reaching from the weir Geesthacht (about 50 km downstream) until Cuxhaven. An inflow boundary condition is given by the gauge station Schöna at the German—Czech border, which includes the whole drainage area of the Czech part of the Elbe catchment which covers an area of about 51000 km². In the south and in the west of the Elbe river basin, the headwaters of the Mulde and Saale catchment are located in the medium range mountains Erzgebirge, Fichtelgebirge and Harz. Annual mean precipitation in the headwaters is between 1000 mm y^{-1} and 1400 mm y^{-1}, mean annual runoff, or discharge goes up to 500–600 mm y^{-1}. In the neighbouring low mountain area regions of Mulde and Saale, the corresponding values are 700–800 mm y^{-1} for the Mulde and 600–700 mm y^{-1} for

the Saale for mean annual precipitation. Long term means for the whole Saale catchment at the gauge station Calbe-Grizehne (see Fig. 1) are 630 mm y^{-1} precipitation and about 150 mm y^{-1} discharge. For the Mulde catchment at Bad Düben, mean precipitation amounts to 770 mm y^{-1} and discharge to 300 mm y^{-1}. The Mulde catchment is prone to flooding. In the northeast, the Havel-Spree catchment is a typical lowland river system in a glacial valley. The Spree river is totally canalized. The Havel river is characterized by a system of connected lakes and channels. Long term mean values for total precipitation are in the range of 500-600 mm y^{-1}, mean discharge is about 120 mm y^{-1}. (Deutsches Gewässerkundliches Jahrbuch, Elbegebiet Teil I-III, 1991, 1992, 1993).

For the atmospheric forcing, a dataset of more than 40 climate stations (DWD, 1994) was used; this comprised daily values of precipitation, air pressure, air temperature, wind speed, humidity and sunshine duration from 1984 up to 1993. An additional dataset from about 150 daily rainfall measurement stations from 1991 up to 1993 was added. For each grid cell, the closest station value was chosen ; for grid cells with more than one station, the values were averaged. Temperature and pressure were adjusted to the mean height of the grid box and a lapse rate of –6.5 °K km^{-1} was used for the temperature and a temperature dependent scale height for the pressure. The vegetation and soil characteristics such as leaf area index, roughness length, saturated hydraulic conductivity, soil texture and displacement height were taken from the data base of the REMO model, which is based on the weather forecast model of the German Weather Service (Majewski, 1991). A minimum canopy resistence was assigned to the vegetation following Shuttleworth (1993). These parameters have not been calibrated in the model runs, as they represent knowledge of the physical system. It is appreciated that an independent parameter study (see Bastidas, 1998) is needed to evaluate the model sensitivity to these parameters and to optimize the model's performance.

Because no root density distribution was available, 50 % of the roots were assigned to each layer. The upper soil layer is approximately half as thick as the lower layer; this correponds to a higher root density in the upper layer.

Starting values for the parameters which are open to calibration (surface runoff parameters (Eqn. 2), Arno baseflow parameters (Eqn. 3), W_2^S d_1, d_2, K and the maximum soil moisture of the two layers) were chosen to be in the mid-range of the parameters from a similar study over the Weser river (Lohmann *et al.*, 1998b).

For the routing procedure, a grid network was set up over the model area (Fig. 3a). Water flows in an unidirectional way from one grid box to the next, where eight directions are possible. Values for the velocity C and diffusivity D were found with the help of river geometry data at gauges along the river network.

Calibration

Parameters for the LSS which were calibrated are the infiltration capacity shape parameter s (Eqn. 1) and the maximum soil moisture in the upper and lower soil layer W_1^{max} *and* W_2^{max} (Eqns. 2 and 3). The baseflow parameters were kept constant during the calibration period, as calibration of these parameters did not improve the streamflow predictions.

For the routing scheme, the Unit Hydrograph was calibrated for each catchment where measured discharge and precipitation are available, with the help of the parameters b and k. The computational procedure for calibration of the coupled hydrological scheme can be seen in Fig. 2. A first guess of the parameters b and k can be estimated from measured discharge in periods with small fast flow. Its purpose is to separate measured discharge into fast flow and slow flow (see Eqn. 5). Fast flow is used in Eqn. 6 to calculate the Unit Hydrograph by an iterative procedure. This Unit Hydrograph is then used to convolute the sum of the VIC-2L surface runoff and baseflow and transport it to the outlet of one grid box. Calibration of the baseflow separation is done by comparison of calculated slow and fast flow from the baseflow separation with the convoluted sum of baseflow and surface runoff from the VIC-2L model. The VIC-2L model is calibrated to match the measured streamflow (Lohmann *et al.*, 1998a, b), while the baseflow separation parameters (b and k) are calibrated so that the slow flow approximates the VIC-2L baseflow and the fast flow matches the VIC-2L surface runoff.

Simulation of water balance and river flow

RESULTS FOR DIFFERENT TIMESCALES

Figures 3, 4 and 5 show the results for a yearly, monthly and daily timescale. In Fig. 3b–3d, there are annual gridded sums of precipitation, evapotranspiration and total runoff as a mean of the period 1991–1993, showing the spatial variation over the whole area. Yearly precipitation ranges from less than 500 mm in the lower areas of Saale and Elbe up to 1140 mm in mountainous regions, in accordance with the long-term climatology. The yearly mean of precipitation over the whole region was about 580 mm. Corresponding values for runoff and evapotranspiration were about 145 mm and 430 mm, respectively; total runoff ranged from 90 mm to 510 mm and evapotranspiration from 340 mm to 630 mm. The ratio of runoff to precipitation ranges from 0.20 in the lower Elbe region to 0.50 in the mountainous regions, with a mean of about 0.25. Table 1 shows the overall results of the simulation for the years 1986 up to 1993. For all 13 gauge stations (for the location see Fig. 1), Table 1 shows yearly means of precipitation, evapotranspiration and calculated and measured discharge in mm y^{-1}. In the Mulde catchment, high rainfall corresponds to high runoff. Lowest rainfall and lowest runoff

Table 1. Annual mean values of the water budget and statistics for calculated and measured runoff in the time period 1986–1993 for 13 catchments.

RIVER Gauge Station	Catchm. area [km^2]	Precipitation [mm y^{-1}]	Evapotranspiration [mm y^{-1}]	Calculated runoff [mm y^{-1}]	Measured runoff [mm y^{-1}]	Correlation coefficient
ELBE						
Neu-Darchau	131950	621	451	167	154	0.92
Magdeburg	94949	631	454	174	173	0.93
SAALE						
Calbe Grizehne	23719	611	440	169	144	0.82
Oberthau	4930	612	462	147	152	0.75
Laucha-Unstrut	6218	712	470	240	191	0.83
Naumburg	11449	644	450	191	176	0.83
Hadmersleben	2758	586	408	178	133	0.72
MULDE						
Bad Düben	6171	747	497	247	292	0.85
Wechselburg	2107	783	516	264	285	0.78
Erlln	2982	790	506	281	333	0.80
SCHW. ELSTER						
Löben	4372	593	457	132	121	0.87
HAVEL/SPREE						
Ketzin	16173	580	435	142	126	0.67
Havelberg	24037	585	440	143	125	0.68

are found in the catchment of Havel/Spree and Schwarze Elster. Table 1 contains also the correlation between measured and calculated discharge for the years 1986–1993. There is a poor correlation ($r < 0.7$) in the Havel/Spree catchment, because the river system is highly canalized. Three smaller catchments show lower correlation ($0.7 < r < 0.8$), whereas in the other catchments correlation is higher than 0.8 and implies a good agreement between measurements and model results.

Figure 4 shows monthly means of the main terms of the water balance over the whole Elbe region for the time period 1986-1993. Figure 4a shows the yearly variation of mean discharge, observed and simulated evapotranspiration and precipitation on a monthly timescale. Maximum precipitation takes place in June, July and December while minimum precipitation occurs in February, April and October. Evapotranspiration has its maximum value in May, but there are also high values in June to August. This means that high precipitation coincides with high evapotranspiration and low mean discharge from May until October.

Discharge is high in winter and spring from December to April, but does not show a clear maximum. In Fig. 4b, monthly variation of soil moisture for layer 1 (the surface layer) and layer 2 (the bottom layer) is shown. Minima for the surface layer are found during May to August, coinciding with high values of evapotranspiration, in spite of high precipitation. Maxima for the bottom layer are in March and April coinciding with high discharge. Minimum values for the bottom layer occur in September and October. From October onwards, percolation from the upper to the lower layer exceeds the continous baseflow, causing an increase in the soil moisture of the lower layer until March/April.

The model results at the outlet of the main catchments and for the time period 1986 up to 1993 on a daily timescale are shown in Fig. 5a for the gauge station Magdeburg, with a catchment area of about 94500 km^2, including the catchments of the river Saale, Mulde and Schwarze Elster and in Fig. 5b for the gauge station Neu-Darchau with a catchment area of about 131950 km^2, including the whole area. Daily means of measured and simulated discharge are shown. 1992 was chosen as a calibration period. Although there is a good agreement in the temporal behaviour, there is some lack of correspondence in winter periods and early spring when snow processes and frozen soil are important.

EXTREME FLOOD EVENTS

The assumption of linear routing is less accurate for high discharge events. Figure 6a shows a scatter plot of all

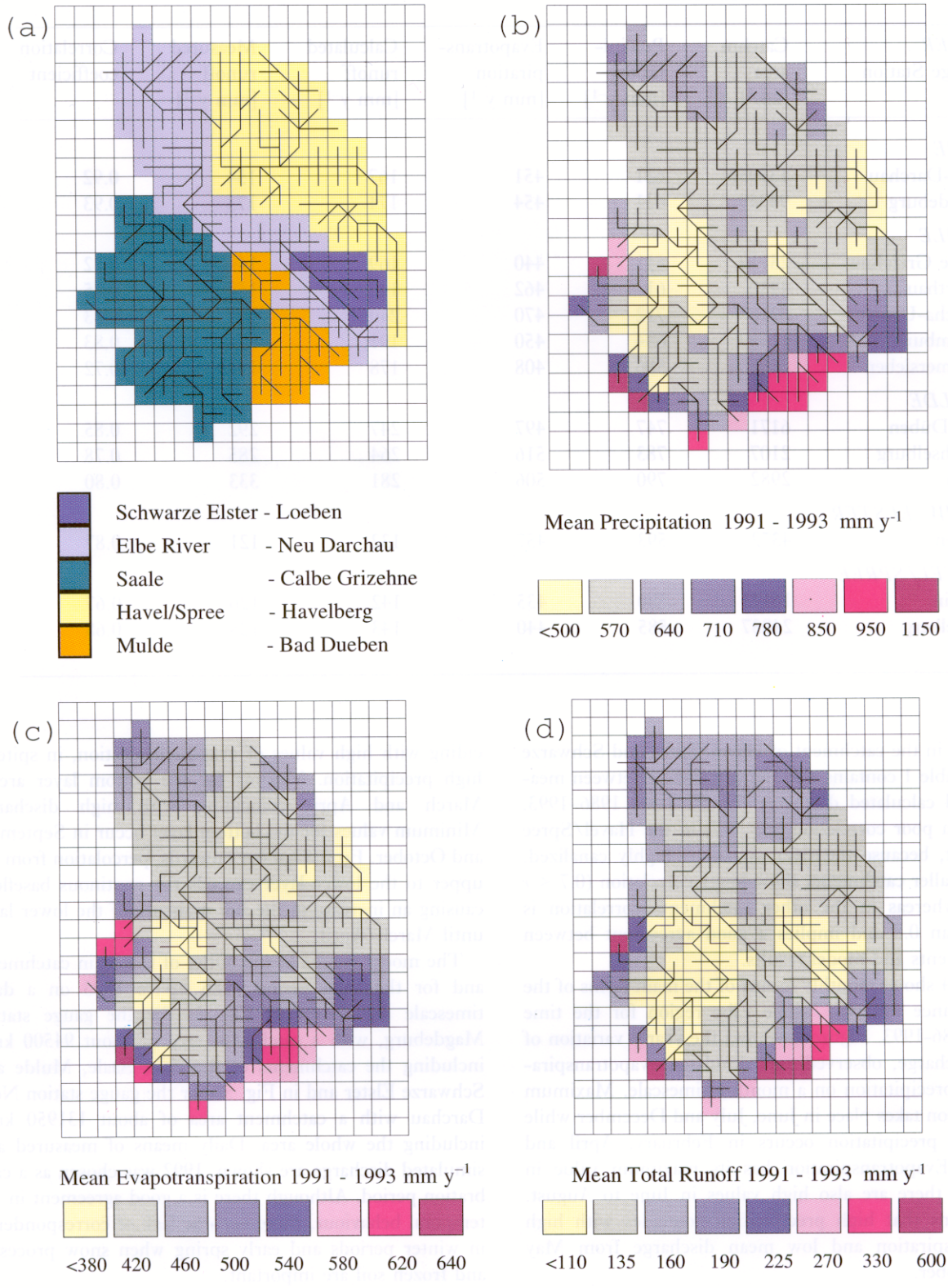

Fig. 3 (a) *Grid network for the model area with main sub-catchments.* (b) *Mean annual rainfall 1991-1993. Units are mm* y^{-1}. (c) *Mean annual evapotranspiration 1991–1993. Units are mm* y^{-1}. (d) *Mean annual total runoff 1991-1993. Units are mm* y^{-1}.

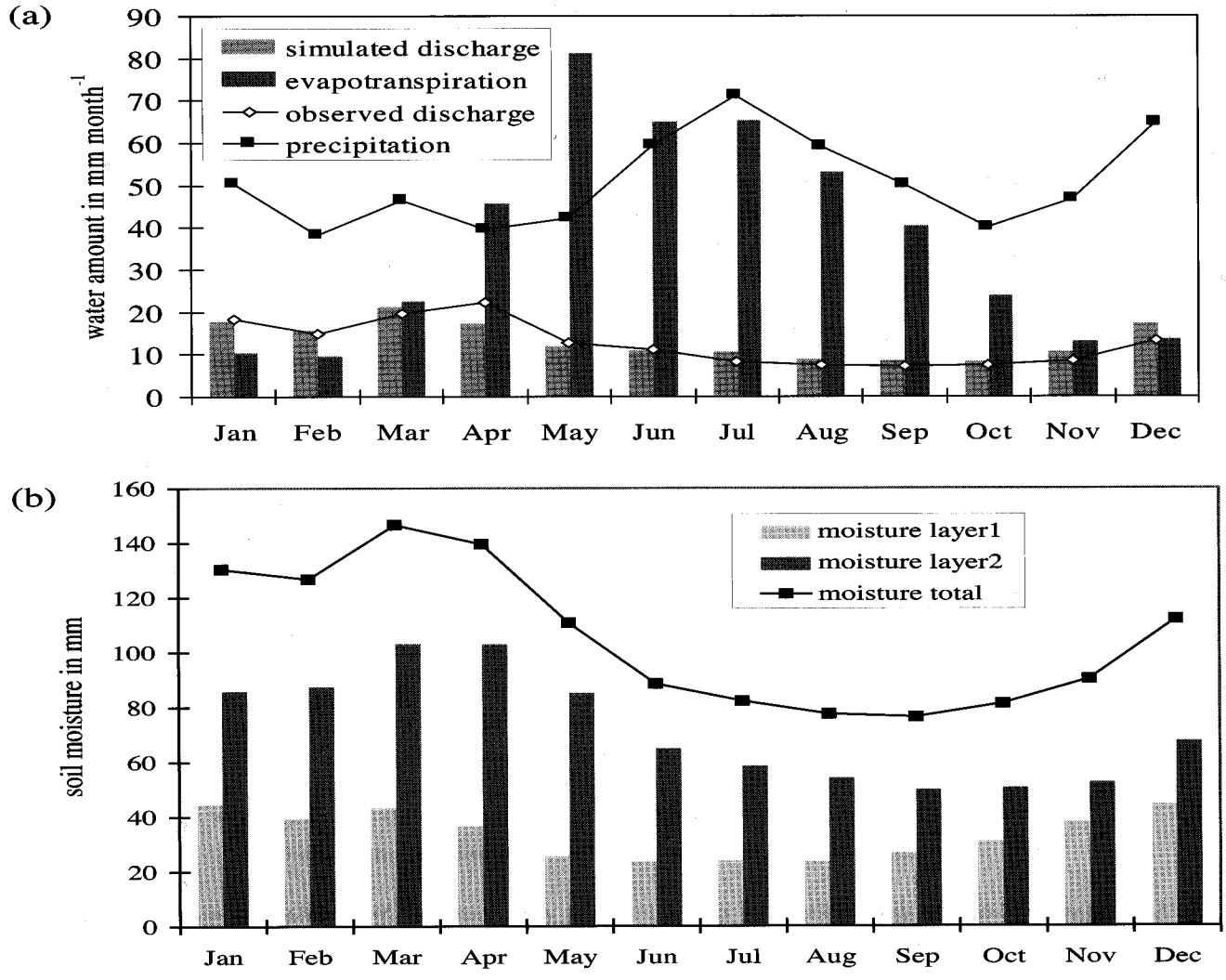

Fig. 4. *Monthly total mean values for the entire Elbe catchment of* (a) *observed and simulated discharge, evapotranspiration and precipitation.* (b) *soil moisture layer 1, soil moisture layer 2 and total soil moisture.*

simulated discharges against the measurements at the gauge station Magdeburg. Beyond values of about 2000 $m^3 s^{-1}$, there are large deviations between the corresponding values of simulated and measured discharge. For the simulation period, there were two flood events with a maximum value greater than 2000 $m^3 s^{-1}$.

The first event occurred between December 1986 and January 1987. Simulated and measured discharge curves at Magdeburg are shown in Fig. 7a. The maximum and the mean discharge for the flood event are both overestimated because of an overestimation in respect of the whole Saale catchment at the gauge station Calbe-Grizehne, with an area of 23700 km^2. It is balanced by an underestimate of discharge for the following time interval up to March 1987; this leads to an underestimate at the gauge Magdeburg. Averaged over the whole period, however, there is a good correspondence of the water balance for both gauges.

These two sequential periods of over- and underestimation also explain the relatively high deviations in Fig. 6a at discharge values below 2000 $m^3 s^{-1}$ (some of these values are marked by open squares). The same effect is seen in Fig. 7b which compares measured and simulated discharge at the gauge Neu-Darchau, which adds an additional area of 37000 km^2 to the catchment above the gauge Magdeburg.

Large differences between measured and simulated discharge between December 1986 and January 1987 are cancelled out by averaging over the whole time period from December 1986 until March 1987. These differences can be explained by looking at the water balance. Figure 6b shows a scatter plot of measured discharge of Magdeburg and Havelberg (including the whole Spree/Havel catchment) routed to the gauge station Neu-Darchau against measured discharge at the gauge station Neu-Darchau. As expected, there is a linear regression of almost unity, the constant

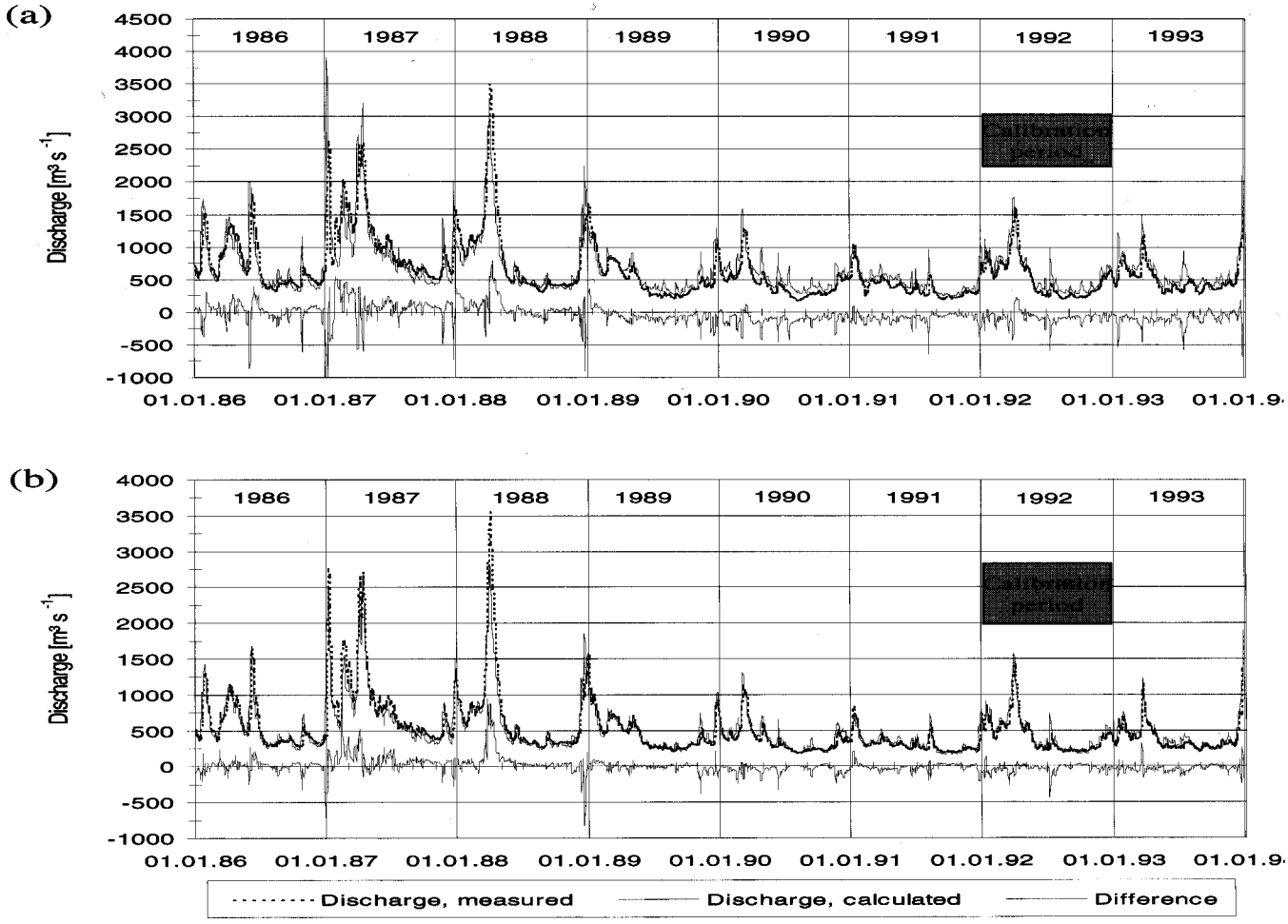

Fig. 5. *Measured and calculated daily discharge and their differences at gauge station* (a) *Neu-Darchau, catchment area 131950 km².* (b) *Magdeburg, catchment area 94949 km².*

Table 2. Comparison of discharge values [$m^3 s^{-1}$] during two flood events (17.12.86–7.3.87 (A), 8.3.88–8.5.88 (B)) for several gauge stations along the Elbe river.

	Catchment area discharge [km²]	maximum discharge (A)	mean discharge (A)	mean discharge (A)	maximum discharge (B)	mean discharge (B)
Date		31.12.86–24.1.87	17.12.86–7.3.87	31.12.86–24.1.87	8.3.88–8.5.88	8.3.88–8.5.88
gauge Calbe-Grizehne	23719	457	240	278	583	349
sim. Calbe-Grizehne	23719	853	226	422	497	281
gauge Barby	94060	2596	1120	1448	3180	1613
gauge Magdeburg	94949	2750	1132	1437	3562	1692
simulation Magdeburg	94949	3224	1100	1728	3107	1515
gauge Tangermünde	97780	2560	1150	1450	3203	1642
gauge Wittenberge	123532	2734	1417	1644	3250	1883
gauge Neu-Darchau	131950	2630	1340	1418	3483	1947
sim. Neu-Darchau	131950	3460	1395	2213	3460	1804
gauge Magdeburg and Havelberg routed	119000	2905	1325	1632	3525	1917

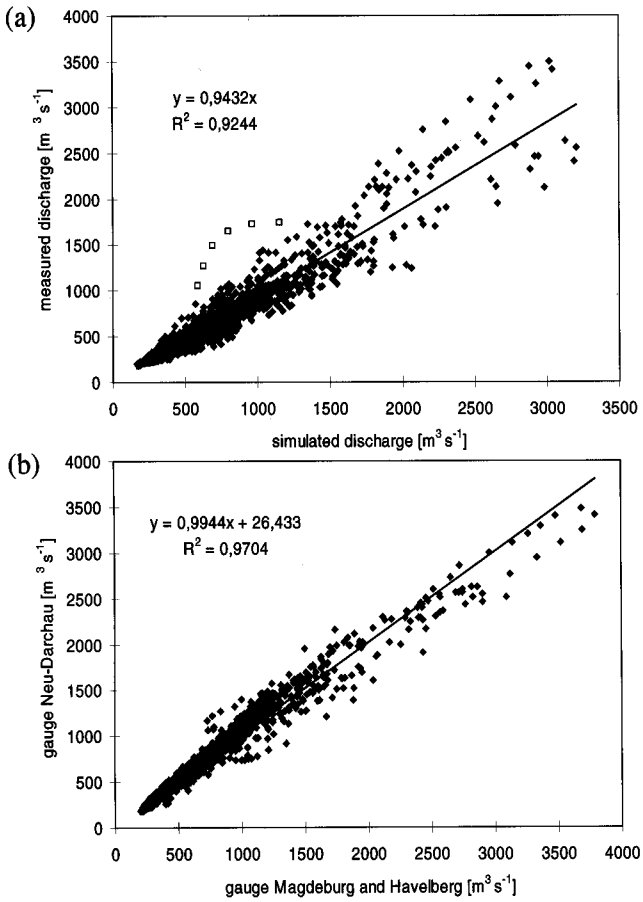

Fig. 6. (a) *Scatterplot of simulated against measured daily discharge at gauge station Magdeburg (1986–93).* (b) *Scatterplot of routed measured discharge from Magdeburg and Havelberg to Neu-Darchau against measured discharge at gauge station Neu-Darchau (1986-93).*

amount of *ca.* 26 $m^3 s^{-1}$ reflects the fact that the catchment area of Magdeburg and Havelberg includes an area which is approximately 5% less than the catchment area of Neu-Darchau. For the flood events, less discharge is measured at Neu-Darchau than is routed from Magdeburg and Havelberg to the gauge station Neu-Darchau. The difference in the water balance is more than 8%; it is even slightly less compared with the gauge station Magdeburg. For the rest of the period, measured and routed discharge agree well within the regression curve. This means, in high discharge events, water is held back in inundation areas (or in bank storage) and, some weeks later, it is added to the discharge. Amount and resident time depend on local effects and the shape of the river bed, as well as the temperature. In January 1987, for almost 3 weeks the mean temperature was about –10 °C and minimum temperature about –20 °C. In addition river discharge may be influenced by ice drift and discharge measurements for these conditions can be in error. For all gauge stations there is a calibrated relationship between water level and discharge. Discharge values are obtained from water level measurements. This relationship is disturbed under conditions of ice formation.

The second flood event is a typical consequence of heavy rainfall and a large amount of water from snowmelt processes. The runoff ratio was about 1.5 from March 1988 until the first week of May 1988 (Table 2). There is an underestimation of more than 10 % in the maximum discharge and the mean discharge at the gauge Magdeburg. To verify the measurements at the gauge Magdeburg, they were compared with the measurements of two neighbouring gauges, one upstream at Barby, with a catchment area which is slightly smaller by 1% and one downstream at Tangermünde, with a catchment area about 3% larger. For these two neighbouring gauges, the maximum discharge is considerably smaller and fits the simulation better. Mean discharge for the whole period is shown in Fig. 8 and also Table 2. The water amount at the gauge Magdeburg is again larger than the water amount at the neighbouring gauges. The simulation underestimates all values by about 5 %.

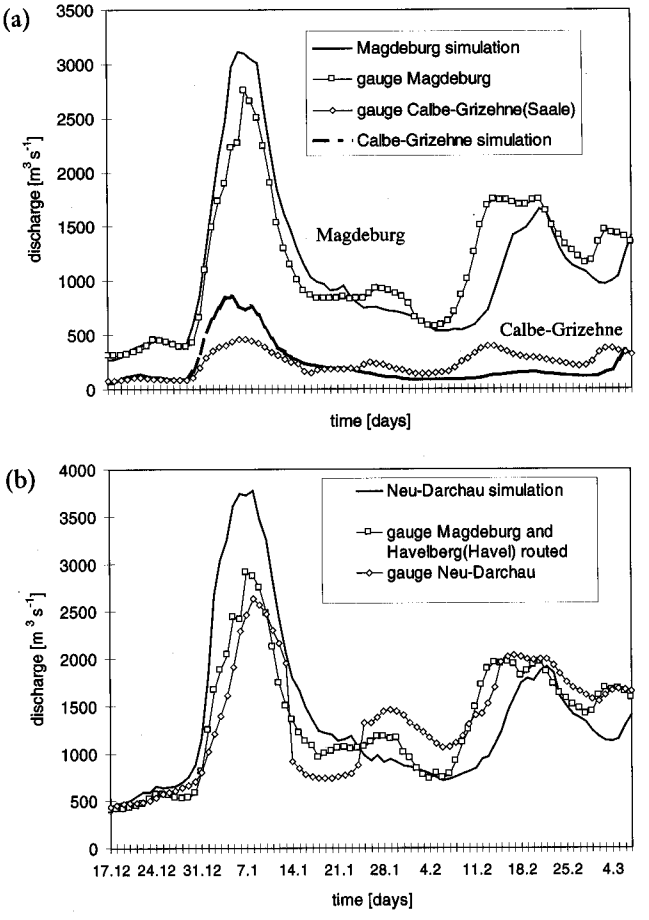

Fig. 7. *Comparison of daily discharge during the flood event 12. 86—1. 87 at gauge station* (a) *Magdeburg.* (b) *Neu-Darchau.*

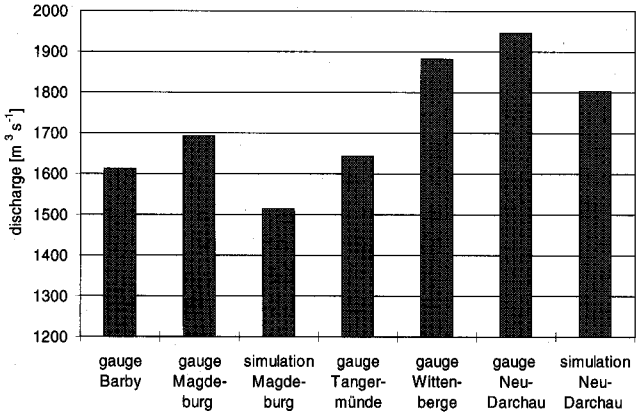

Fig. 8. *Comparison of mean discharge values during the flood event 8.3.88-8.5.88 at several gauge stations along the Elbe river.*

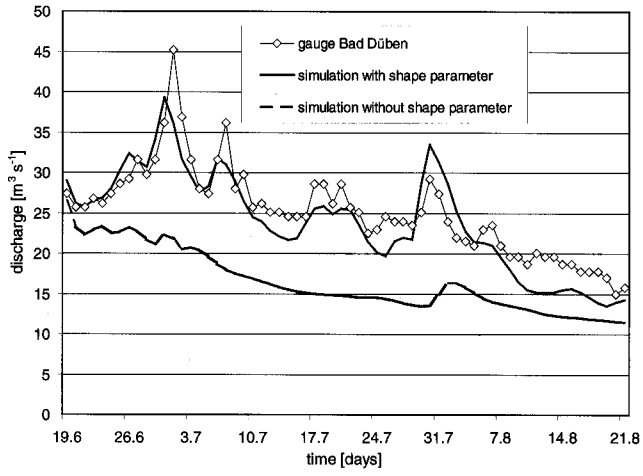

Fig. 9. *Discharge at gauge Düben (Mulde catchment) 19.6.88—21.8.88. Comparison simulation without shape parameter and with an appropiate calibrated shape parameter.*

Here, in addition to errors in the input forcing data, parametrizations and gridding procedures, there may also be errors in the discharge measurements, primarly in flood events. An adequate routing scheme for flood events has to take into consideration the processes of inundation areas; therefore detailed treatment of the nonlinear St. Venant's equation (Fread, 1993) will be necessary, as well as the inclusion of bank storage effects.

INFLUENCE OF THE SHAPE PARAMETER

By investigating the behaviour of the calibration procedure the influence of the shape parameter in Eqn. 1 on runoff and evapotranspiration is tested. Simulation of the water balance without the shape parameter over the whole time period for the gauge Magdeburg leads to less runoff production about 10 mm y^{-1}, causing more evapotranspiration of about 10 mm y^{-1}. Also the correlation coefficient between measured and simulated discharge diminishes. Without the shape parameter, a simple 'bucket model' for the upper layer assumes that all rainfall is infiltrated until the soil moisture capacity is exceeded, whereafter the excess precipitation becomes runoff. Time and amount of surface runoff as response to a precipitation event is different compared with the VIC model and also compared to measurements. An example can be seen in Fig. 9. Discharge at the gauge Bad Düben (Mulde catchment) is shown for a relatively dry summer period from 19.6.88 to 4.10.88. mean measured discharge is about 25 $m^3 s^{-1}$, simulation without the shape parameter leads to a mean discharge of about 17 $m^3 s^{-1}$ and no correlation, whereas simulation with an appropiate calibrated shape parameter leads to a mean discharge of about 24 $m^3 s^{-1}$ and a correlation coefficient of 0.9. The runoff response to a precipitation event follows the measured curve, in the case of the calibrated shape parameter, whereas without the shape parameter there is no surface runoff, because the maximum storage capacity of the upper layer is not yet reached .

Conclusions

A grid version of a LSS, describing vertical water movement and soil vegetation atmosphere interaction inside each grid cell is used. Atmospheric forcing is done by measured daily mean values of precipitation, air temperature, humidity, pressure, wind speed and sunshine duration. A linear routing scheme is used to describe the horizontal water movement. Surface runoff and baseflow were routed inside each grid box, using a simple Unit Hydrograph scheme. Water is transported between neigbouring grid boxes by river routing, using the solution of the linearized St. Venant's equation. By comparing measured and simulated discharge at the catchment outlet, a calibration procedure is set up, with the maximum soil water content and the shape parameter of the infiltration curve of the LSS being subject to calibration.

Measured and simulated discharge at the outlet of the whole area and at the outlet of the subcatchments are in agreement within the range of 0.95 and 0.7 for the correlation coefficient (Table 1). Important processes and terms of the water balance can be explained on a daily, monthly and annual timescale for the whole basin but also for different subcatchments. Some discrepancies between measurements and modelled results are shown for time periods where snow processes and frozen soil are important. The assumption of linear routing with time independent values for the velocity, C, and diffusivity, D, is sufficient on daily and longer timescales. For extreme flood events, a more detailed treatment of the nonlinear St. Venant's equation (Fread, 1993) will be necessary.

The parameterizations used in this paper can be easily included in any common LSS. The major differences between the VIC-2L model and many other LSS (such as used in PILPS or the GSWP) are the treatment of the upper and lower boundary conditions (VIC and Arno-

baseflow parameterization) of water fluxes. These parameterizations can be justified with the spatial heterogeneity of soil moisture and simplified solutions of groundwater equations (see Lohmann *et al.*, 1998a). The routing model has already been used with 16 different LSSs in the PILPS phase 2(c) (Lohmann *et al.*, 1998).

With a coupled hydrological model, calibrated for each catchment, numerical studies over large river basins can be performed. An essential requirement is that the results are validated with measured discharge on a daily time scale, otherwise the different mechanisms for runoff production cannot be identified in the model results.

Acknowledgements

The authors wish to thank the Bundesamt für Gewässerkunde (BfG), Berlin, the Sächsisches Landesamt für Umwelt und Geologie, the Landesumweltamt Brandenburg, the STAU (Staatliches Umweltamt) Halle and the STAU Magdeburg for providing streamflow data. They also thank the German Weather Service (DWD) for providing precipitation and synoptical data.

References

Bastidas, L.A., 1998. *Parameter Estimation for Hydrometeorological Models using Multi-Criteria Methods,* Ph.D. dissertation, Department of Hydrology and Water Resources, The University of Arizona, Tucson, AZ 85721

Brooks, R.H. and Corey, A.T., 1988. *Hydraulic Properties of Porous Media.* hydrol. Pap., Colorado State University, p. 3.

Burnash, R.J.C., 1995. The NWS River Forecast System-Catchment Modeling. In: Singh, V.P. (ed.), *Computer Models of Watershed Hydrology*, Water Resources Publications, 311–366.

Chen, T.H.J., Henderson-Sellers, A., Milly, P., Pitman, A., Beljaars, A., Abramopoulos, F., Boone, A., Chang, S., Chen, F., Dai, Y., Desborough, C., Dickinson, R., Dümenil, L., Ek, M., Garratt, J., Gedney, N., Gusev, Y., Kim, J., Koster, R., Kowalczyk, E., Laval, K., Lean, J., Lettenmaier, D., Liang, X., Mahfouf, J., Mengelkamp, H.-T., Mitchell, K., Nasonova, O., Noilhan, J., Polcher, J., Robock, A., Rosenzweig, C., Schaake, J., Schlosser, C., Schulz, J.P., Shao, Y., Shmakin, A., Verseghy, D., Wetzel, P., Wood, E., Xue, Y., Yang, Z.L., and Zeng, Q., 1997. Cabauw Experimental Results from the Project for Intercomparison of Landsurface Parametrization Schemes (PILPS), *J. Climate,* **10**, 1194–1215.

Deutsches Gewässerkundliches Jahrbuch, Elbegebiet Teil I, II,III, 1991, 1992, 1993. Landesamt für Umweltschutz Sachsen-Anhalt (Teil I), Halle (Saale), Landesumweltamt Brandenburg (Teil II), Frankfurt (Oder), Wirtschaftsbehörde Strom und Hafenbau (Teil III), Hamburg.

Duband, D., Oblet, C. and Rodriguez, J.Y., 1993. Unit hydrograph revisited: an alternative iterative approach to UH and effective precipitation idendification. *J. Hydrol.*, **150**, 115–149.

DWD, 1994. Die Datenarchive der operationellen NW-Modelle des Deutschen Wetterdienstes, Deutscher Wetterdienst Offenbach.

Francini, M. and Pacciani, M., 1991. Comparative analysis of several conceptual rainfall-runoff models. *J. Hydrol.*, **122**, 161-219.

Fread, D.L., 1993. Flow routing. In: Maidment, D.R. (ed), *Handbook of Hydrology*, Ch. 10, McGraw Hill.

Gray, D.M. and Prowse, T., D., 1993. In: Maidment, D.R. (ed), *Handbook of Hydrology*, Ch. 7, McGraw Hill.

Gupta, V.K., Rodriguez-Iturbe, I. and Wood, E.F., 1986. *Scale Problems in Hydrology*, D. Reidel Publishing Company, Dordrecht, Netherland, 5–11.

GSWP, 1998. Global Soil Wetness Project, Preliminary Report on the Pilot Phase, International GEWEX Project Office (IGPO) Publication Series No. 29.

Henderson-Sellers, A. and Hopkins L. (ed.), 1998. Coupling Land and Atmosphere, Special Issue, *Global and Planetary Change*, **19**.

Henderson-Sellers, A., Pitman, A.J., Love, P.K., Irannejad, P. and Chen, T.H., 1995. The Project for intercomparison of Land-surface Parametrization Schemes (PILPS); phases 2 and 3; *Bull. Am. Meteorol. Soc.* **76**, 489–503.

Karstens, U., Nolte-Holube, R., and Rockel, B., 1996. Calculation of the water budget over the Baltic Sea catchment area using the regional forecast model REMO for June 1993. *TELLUS*, **48A**, 684–692.

Liang, X., 1994. *A two-layer variable infiltration capacity land surface representation for general circulation models.* Water Resources Series, Technical report No. 140, Department of Civil Engineering, University of Washington.

Liang, X., Lettenmaier, D.P., Wood, E.F. and Burges, S.J., 1994. A simple hydrologically based model of land surface water and energy fluxes for general circulation models. *J. Geophys. Res.*, **99**, **D3**, 14415–14428.

Liang, X., Lettenmaier, D.P., Wood, E.F., Lohmann, D., Boone, A., Chang, S., Chen, F., Dai, Y., Desborough, C., Dickinson, R.E., Duan, Q., Ek, M., Gusev, Y., Habets, F., Irannejad, P., Koster, R., Michell, K., Nasonova, O.N., Noilhan, J., Schaake, J., Schlosser, A., Yaping, S., Shmakin, A., Verseghy, D., Warrach, K., Wetzel, P., Xue, Y., Yang, Z.L. and Zeng, Q., 1998. The Project for Intercomparison of Land-Surface Parametrization Schemes (PILPS) Phase 2c, Red-Arkansas River basin Experiment: 2. Spatial and temporal analysis of energy fluxes. *Global and Planetary Change*, **19**, 137–159.

Lohmann, D., Nolte-Holube, R. and Raschke, E., 1996. A large scale horizontal routing model to be coupled to land surface parametrisation schemes. *TELLUS*, **48A**, 708-721.

Lohmann, D., Raschke, E., Nijssen, B. and Lettenmaier, D.P., 1998. Regional scale hydrology: I. Formulation of the VIC-2L model coupled to a routing model. *Hydrol. Sci. J.* **43** 131–141.

Lohmann, D., Raschke, E., Nijssen, B. and Lettenmaier, D.P., 1998. Regional scale hydrology: II. Application of the VIC-2L model to the Weser River, Germany. *Hydrol. Sci. J.* **43** 143–158.

Lohmann, D., Lettenmaier, D.P., Liang, X., Wood, E.F., Boone, A., Chang, S., Chen, F., Dai, Y., Desborough, C., Dickinson, R.E., Duan, Q., Ek, M., Gusev, Y., Habets, F., Irannejad, P., Koster, R., Michell, K., Nasonova, O.N., Noilhan, J., Schaake, J., Schlosser, A., Yaping, S., Shmakin, A., Verseghy, D., Warrach, K., Wetzel, P., Xue, Y., Yang, Z.L. and Zeng, Q., 1998. The Project for Intercomparison of Land-Surface Parametrization Schemes (PILPS) Phase 2c Red-Arkansas River basin Experiment: 3. Spatial and temporal analysis of water fluxes. *Global and Planetary Change*, **19**, 161–179.

Majewski, D., 1991. *The Europamodell of the Deutscher Wetterdienst.* In: ECMWF Course 'Numerical Methods in atmospheric Models', Vol. 2, 147–191.

Moussa, R. and Bocquillon C., 1996. Criteria for the choice of flood-routing methods in natural channels . *J. Hydrol.* **186**, 1–30.

Nijssen, B. and Lettenmaier, D. P., Liang, X., Wetzel, S.W., Wood, E.F., 1997. Streamflow simulation for continental-scale river basins. *Wat. Resour. Res.* **33**, 711–721.

Noilhan J. and Planton, S., 1989. A simple parameterization of land surface processes for meteorological models. *Mon. Wea. Rev.*, **117**, 536–549.

O'Connell, P.E. and Todini, E., 1996. Modelling of rainfall flow and mass transport in hydrological systems: an overview. *J. Hydrol.*, **175**, 3–16.

Raschke, E., Karstens, U., Nolte-Holube, R., Brandt, R., Isemer, H.J., Lohmann, D., Lobmeyr, M., Rockel, B. and Stuhlmann, R., 1998. The Baltic Sea experiment BALTEX: A brief overview and some selected results of the authors, *Surveys in Geophysics* **19**, 1–22.

Rodriguez, J.Y., 1989. *Modelisation pluie-debit par la methode DPFT.* These de doctorat, Grenoble, France.

Shuttleworth, W.J., 1993. Evaporation. In: Maidment, D.R.(ed.), *Handbook of Hydrology*, Chap. 4, McGraw Hill.

Todini, E., 1991. Hydraulic and Hydrological Flood Routing Schemes. In: Bowles, D.S., O'Connell, P.E. (ed.), *Recent Advances in the modeling of Hydrologic Systems*, NATO ASI Series C, Vol. 345, 389–406.

Wood, E.F., Lettenmaier, D.P. and Zartarian, V.G., 1992. A land surface hydrology parametrization with subgrid variability for general circulation models. *J. Geophys. Res.*, **97, D**, 2717–2728.

Wood, E.F., Liang, X., Lettenmaier, D.P., Lohmann, D., Boone, A., Chang, S., Chen, F., Dai, Y., Dickinson, R.E., Duan, Q., Ek, M., Gusev, Y., Habets, F., Irannejad, P., Koster, R., Michell, K., Nasonova, O.N., Noilhan, J., Schaake, J., Schlosser, A., Yaping, S., Shmakin, A., Verseghy, D., Warrach, K., Wetzel, P., Xue, Y., Yang, Z.L. and Zeng, Q., 1998. The Project for Intercomparison of Land-Surface Parametrization Schemes (PILPS) Phase 2c, Red-Arkansas River basin Experiment: 1. Experiment description and summary intercomparisons. *Global and Planetary Change*, **19**, 115–135.